Journal of Food Engineering 369 (2024) 111909

Contents lists available at ScienceDirect

Journal of Food Engineering

journal homepage: www.elsevier.com/locate/jfoodeng

Development and validation of engineering charts: Heating time and optimal salt content prediction for microwave assisted thermal sterilization

Yonas Gezahegn [a], Juming Tang [a,*], Patrick Pedrow [b], Shyam S. Sablani [a], Zhongwei Tang [a], GustavoV. Barbosa-Cánovas [a,c]

[a] Department of Biological Systems Engineering, Washington State University, P.O Box 646120, Pullman, WA, 99164-6120, USA
[b] School of Electrical Engineering & Computer Science, Washington State University, P.O Box 642752, Pullman, WA, 99164-2752, USA
[c] Center for Nonthermal Processing of Food, Washington State University, Pullman, WA, 99164, USA

ARTICLE INFO

Keywords:
Dielectric properties
Engineering chart
Formulation
Heating time
Microwave processing
Sterilization

ABSTRACT

Through decades of research and development efforts, Microwave Assisted Thermal Sterilization (MATS) systems started commercial operation for production of shelf-stable meals in 2019. It is now highly desirable to develop user-friendly tools to facilitate the development of commercial MATS processes. The aim of this research was to develop engineering charts by applying Maxwell's and heat transfer equations to illustrate the relationships among dielectric properties, temperature, salt content, product thickness and heating rate for microwave heating in a MATS system. Three G-T (Gezahegn-Tang) charts were developed for mashed potato, peas, and rice products with MATLAB software. The charts can be used to determine the heating temperature, time and optimum salt content for a maximum heating rate at the center of a product. Experimental validation tests using mashed potato samples confirmed that the temperature profiles measured at the cold spots of the samples in the microwave heating section of the MATS system were positively correlated with predicted temperatures from the chart (R^2 = 0.94–0.99). Furthermore, the predicted optimal salt contents for 23 mm thick mashed potato (0.1%), 18 mm thick pea (0.5%) and 25 mm thick rice (1%) samples agreed with the experimental heating pattern test results. The optimal salt content is inversely proportional with a product temperature and thickness, which increases the microwave power decay before reaching the center. With the help of these charts, the food industry practitioners can save significant time and resources during the development of food products and schedules for the MATS processes.

1. Introduction

Ready-To-Eat (RTE) meals are defined as prepared foods that can be consumed immediately or with minimal preparation (Remnant and Adams, 2015). Consumption of RTE meals has considerably increased over the last few decades due to the busy lifestyle of the population that led to increased market demand for RTE meals (Hillier-Brown et al., 2017; Thienhirun and Chung, 2018). A Harvard Business Review paper by Yoon (2017) reported that only 10% of American consumers enjoy to cook at home; whereas most Americans buy RTE meals or serves in restaurants. Although RTE meals are popular these days, producing safe and high-quality shelf stable RTE meals is a challenge for the food industry. Therefore, effective technologies are needed for safe commercial production of RTE meals (Tang et al., 2018).

After over 20 years of research and development as described by Tang (2015), Microwave Assisted Thermal Sterilization (MATS) systems (Fig. 1) are now used for the commercial production of shelf-stable RTE meals in industries such as "Tata SmartFoodz Limited." This technology is based on a 915 MHz single-mode designed and developed at Washington State University (WSU), USA. Compared to conventional surface heating methods, the MATS capability to volumetrically heat foods sharply reduces processing time, resulting in less quality degradation and nutritional losses (Chizoba Ekezie, Sun, Han and Cheng, 2017; İcier and Baysal, 2004; Tang, 2015). Fig. 1 illustrates the diagram of a pilot MATS system, which has served as the basis for the design of MATS systems currently used in the commercial production of RTE meals.

The pilot system consists of four main sections corresponding to four processing stages: preheating, heating, holding, and cooling. In processing, packaged foods are immersed in the circulating water and transported *via* a conveyor through the four sections. In the preheating

* Corresponding author.
E-mail addresses: yonas.gezahegn@wsu.edu (Y. Gezahegn), jtang@wsu.edu (J. Tang).

https://doi.org/10.1016/j.jfoodeng.2023.111909
Received 10 September 2023; Received in revised form 2 December 2023; Accepted 19 December 2023
Available online 20 December 2023
0260-8774/

section, the food reaches an initial preheating temperature before being moved through to the microwave heating section, where the food is heated to a sterilization temperature (118–124 °C). Following microwave heating, the food is moved through the holding section to reach the target lethality for *C. botulinum* spores and is then moved to a cooling section (23 °C) (Hong et al., 2021a,b; Luan et al., 2016; Resurreccion et al., 2013; Tang et al., 2006).

In sterilization process development, the adequacy of heat treatment at the product cold spot (the least heated spot) is critical to fulfill the required process lethality to the target pathogen (FDA, 2016; IFTPS, 2014). Previous studies on MATS reported a robust method to accurately locate the cold spot of various food products with the help of chemical markers (to detect relative heating absorptions) and an image processing program based on IMAQ Vision Builder software (to capture and analyze color patterns inside the thermally processed food products) (Pandit et al., 2006, 2007). Systematic studies have also been conducted on the performance of mobile metallic sensors for cold spot temperature measurement in food packages (Luan et al., 2013, 2015).

Even though validation tests are mandatory for new sterilization process development for the "Food and Drug Administration" (FDA) filing; having an effective temperature predicting tool at the cold spot is greatly helpful for food companies in reducing process development time (FDA, 2016; IFTPS, 2014). Due to the complex nature of microwave heating, it is particularly desirable to develop engineering charts that relate food dielectric properties and package thickness to heating rates in food packages (Jain et al., 2019; Tang, 2015).

The relative dielectric permittivity (ε_r^*), relative to free space, is one of the critical physical properties that influence microwave heating. This property is defined as:

$$\varepsilon_r^* = \varepsilon'_r - j\varepsilon''_r \tag{1}$$

where j = $\sqrt{-1}$, the relative dielectric constant (ε_r') represents the ability of food to store electric energy, the relative dielectric loss factor (ε_r'') describes the ability of food to convert microwave energy to thermal energy. By convention the relative dielectric properties are often referred to as dielectric constant (ε') and dielectric loss factor (ε''), without the subscript "*r*." The dielectric properties are determined by food compositions (mainly moisture and salt content), temperature and frequency (İcier and Baysal, 2004; Ryynänen, 1995).

As discussed by Hong et al. (2021a,b) and Jain et al. (2019), the thickness of a food product plays a key role in determining the heating rate of the product at the center layer. With increasing product thickness, the power dissipation, and the resulting heating rate at the center of a product decreases.

Due to the importance of a useful tool for predicting a product heating temperature at the center layer, Gezahegn et al. (2023) developed analytical charts that illustrate the relationships among the food dielectric properties, temperature, thickness, and microwave power dissipation during processing in a Microwave Assisted Thermal Pasteurization System (MAPS). However, because of the operating temperature difference between the MAPS (≤91 °C) and MATS (≤124 °C) processes, the analytical charts developed for MAPS are not relevant to the MATS systems. Due to the higher operating temperatures, the dielectric properties of the products and the circulating water in the MATS system are different from those of the MAPS. Additionally, the net microwave power applied in the MATS system (~15 kW) is higher than in the MAPS (~10 kW). Hence, this research aimed to: a) develop engineering charts that show the relationships among the food dielectric properties, temperature, thickness, and microwave power dissipation for predicting the center layer heating rate of packaged food processed in a MATS system; b) validate the chart using a pilot scale MATS system for different food products, dielectric properties and package thicknesses; and c) demonstrate the use of the charts for predicting the microwave heating rate, heating time and determining the optimal salt content formulation for faster heating.

2. Mathematical models

Fig. 2 shows the detailed schematic diagram of a single-mode microwave heating cavity of the MATS system. As stated by Gezahegn et al. (2023), the following assumptions were used to predict the heating rate of a food product in the microwave heating cavity: a) TE_{10} single-mode 915 MHz electromagnetic plane waves entered the horn applicators from the top and bottom waveguides with no phase difference (0°); b) the waves traveled perpendicularly from air through the circulating water to the food; c) the food products were solid, homogeneous,

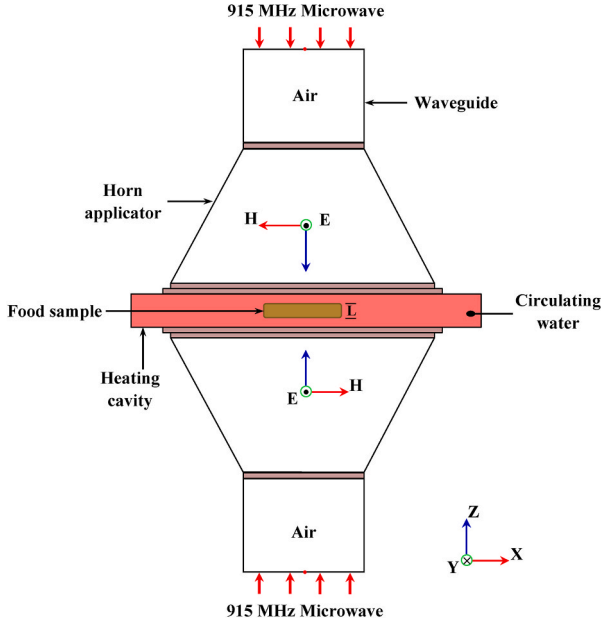

Fig. 2. A single-mode microwave heating cavity with a food sample, L = thickness (adapted from Gezahegn et al. (2023)).

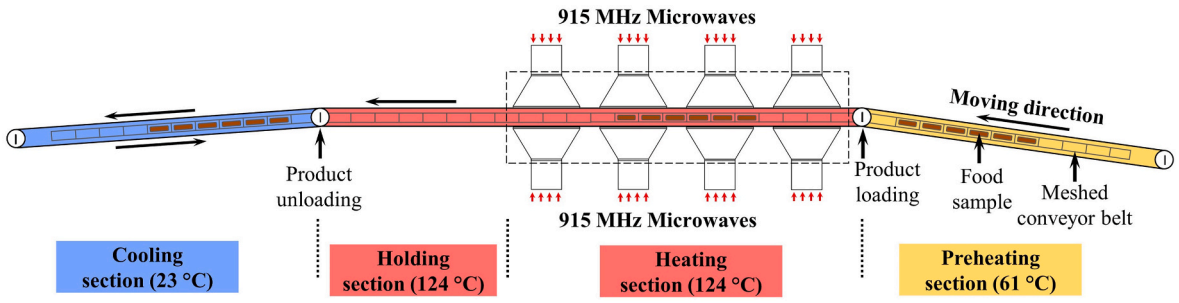

Fig. 1. Schematic diagram of the pilot plant MATS system at WSU.

isotropic, packed in a rectangular-shape polymer container; and d) the microwave power, which has a rapid heat generation, was considered to be the dominant heat source and the conductive heating (relatively slower) from the circulating water to the center of the food was considered negligible for short-time microwave heating (typically 2–5 min).

Based on the above conditions and assumptions, Eq. (2) was developed to quantify the electric field intensity (E, in V/m) inside the food as a function of distance (Z, in m) from the top to the bottom surface of the food along the food thickness (L, in m) (Jain et al., 2019).

$$E = \frac{T_{w/f} E_0}{1 + R_{w/f} e^{-\gamma_f L}} \left(e^{-\gamma_f Z} + e^{-\gamma_f (L-Z)} \right) \tag{2}$$

where E_0 represents the average incident electric field intensity at food surfaces (the interfaces between water and food); T and R represent the transmission coefficient and reflection coefficient, respectively from the circulating water to the food; γ represents the propagation constant; subscript f and w represent the food and water, respectively. The average incident electric field (E_0) was determined with preliminary experiments through reverse calculation (using Eqs. (2) and (13)) from the measured temperature and heating rate profile in mashed potato samples as described by Gezahegn et al. (2023). For all food samples with 16–28 mm thicknesses, E_0 was found to be 0.53 kV/m when the average net microwave power of 15 kW was applied in the four cavities.

The propagation constant (γ) is expressed as:

$$\gamma = \alpha + j\beta \tag{3}$$

where the real part, α (Np/m), is the attenuation constant; and the imaginary part, β (rad/m), is the phase constant. The constants can be calculated from:

$$\alpha = \frac{2\pi f}{c} \sqrt{\frac{\varepsilon'}{2} \left(\sqrt{1 + \left(\frac{\varepsilon''}{\varepsilon'} \right)^2} - 1 \right)} \tag{4}$$

$$\beta = \frac{2\pi f}{c} \sqrt{\frac{\varepsilon'}{2} \left(\sqrt{1 + \left(\frac{\varepsilon''}{\varepsilon'} \right)^2} + 1 \right)} \tag{5}$$

where f and c are frequency and speed of light ($3x10^8$ m/s), respectively (Balanis, 2012). In a lossy medium, the transmission ($T_{w/f}$) and reflection ($R_{w/f}$) coefficients are quantified as:

$$T_{w/f} = \frac{2\eta_f}{\eta_f + \eta_w} \tag{6}$$

$$R_{w/f} = \frac{\eta_f - \eta_w}{\eta_f + \eta_w} \tag{7}$$

where η_f and η_w represent complex intrinsic impedance of the food sample and circulating water, respectively. The intrinsic impedances are expressed as:

$$\eta_f = \frac{\eta_o}{\sqrt{\varepsilon_f^*}} \tag{8}$$

$$\eta_w = \frac{\eta_o}{\sqrt{\varepsilon_w^*}} \tag{9}$$

where η_o is the intrinsic impedance of free space (377Ω), ε_f^* is the electric permittivity of food, and ε_w^* is the electric permittivity of the circulating water (Balanis, 2012).

The microwave power dissipation (P, in W/m^3) and heating rate (dT/dt, in °C/sec) inside the food varying with distance (Z, in m), were calculated by Eqs. (10) and (11), respectively (Balanis, 2012; Jain et al., 2019):

$$P(z) = 2\pi f \varepsilon_0 \varepsilon'' |E|^2 \tag{10}$$

$$\frac{dT}{dt} = \frac{P(z)}{\rho C_P} \tag{11}$$

where ε_0 is the dielectric permittivity of vacuum (8.85×10^{-12} F/m), and ρC_P represents the volumetric specific heat (in J/(°C·m^3)) of the food.

3. Material and methods

3.1. Sample preparations

Mashed potato, peas and rice samples were used to develop and validate the analytical charts. Different salt (food grade, Morton, Chicago, IL, USA) contents were added to vary the dielectric properties of the foods. The mashed potato samples were prepared by mixing 20% (wt/wt) potato flakes (Oregon Potato Company, Pasco, WA, USA) and distilled water along with six salt contents (0, 0.1, 0.2, 0.5, 1 and 2% wt/wt) as described by Jain et al. (2019). The pea samples were prepared by soaking dry white peas (Swad, Skokie, IL) at room temperature overnight and pre-cooking them in distilled water (1.5 times of the pea weight) at 95 °C for 60 min. The peas were ground and six different salt contents (0, 0.1, 0.2, 0.5, 1 and 2% wt/wt) were added. For rice samples, medium-size grains (Nishiki, Los Angeles, CA) were pre-cooked in distilled water (1.2 times of the rice weight) at 95 °C for 40 min. Six different salt contents (0, 0.2, 0.5, 1, 1.5 and 2% wt/wt) were added to the water before cooking (Jain et al., 2019). In all three kinds of samples, 0.5% D-ribose was added as a precursor of the chemical marker M-2 for the purpose of heating pattern detection (Zhang et al., 2014).

3.2. Physical properties measurement

The dielectric properties of all the samples were measured in triplicates at 915 MHz between 20 and 120 °C using an HP 8752C Network Analyzer and an 85070B open-end coaxial dielectric probe (Agilent Technologies, Santa Clara, CA, USA) as described by Gezahegn et al. (2021). The dielectric properties of the circulating water (softened tap water) used in the MATS system were 56 for loss factor and 3 for dielectric constant at 120 °C (Jain et al., 2019; Tang, 2015).

3.3. Validation experiments

3.3.1. MATS processing

For the validation experiments, mashed potato samples of 200 g (16 mm in thickness), 250 g (20 mm), 300 g (23 mm) and 350 g (28 mm) with various salt contents (0, 0.1, 0.2, 0.5, 1 and 2%) were filled into rectangular polymer trays (dimension: 140 × 95 × 30 mm). Pea samples of 300 g (18 mm) with 0, 0.1, 0.2, 0.5, 1 and 2% salt contents and rice samples of 300 g (25 mm) with 0, 0.2, 0.5, 1, 1.5 and 2% salt contents were filled into separate rectangular polymer trays (dimension: 140 × 95 × 25 mm). The trays were vacuum sealed at 6.5 kPa, 195 °C and for 12 s with a Multivac T-200 sealer (Multivac Inc., Kansas City, MO, USA). Before sealing, a mobile temperature sensor (Ellab Inc., Hillerod, Denmark) was embedded in the food sample with its tip located at the cold spot, as described by Luan et al. (2015). The cold spot location in each of products was previously identified by Jain et al. (2019).

The total net power supplied to the heating cavities by the pilot scale MATS system was 15.0 ± 0.2 kW (6, 5.2, 2.4 and 3.2 kW for each cavity). The packages were placed on a conveying belt and preheated to 61 °C by circulating warm water. The samples were then moved through the heating section to be heated by microwaves and by circulating hot water (124 °C) for 4.6 min and through the holding section (124 °C) for 4.7 min. Finally, the samples were moved to the cooling section to reach room temperature (~23 °C). During the process, a gauge pressure of

Table 1
Relationships between temperature T (20–120 °C) and the dielectric loss factor at different salt contents, (n = 3).

Salt content	Correlations	R^2
Mashed Potatoes		
0.0 %	$\varepsilon'' = 3 \times 10^{-4} \times T^2 + 0.1043 \times T + 11.75$	0.99
0.1 %	$\varepsilon'' = 14 \times 10^{-4} \times T^2 + 0.0232 \times T + 16.22$	0.99
0.2 %	$\varepsilon'' = 22 \times 10^{-4} \times T^2 - 0.0225 \times T + 20.52$	0.99
0.5 %	$\varepsilon'' = 15 \times 10^{-4} \times T^2 + 0.1807 \times T + 22.90$	0.99
1.0 %	$\varepsilon'' = 39 \times 10^{-4} \times T^2 + 0.0646 \times T + 37.15$	0.99
2.0 %	$\varepsilon'' = 56 \times 10^{-4} \times T^2 + 0.3904 \times T + 42.76$	0.99
Peas		
0.0 %	$\varepsilon'' = -2 \times 10^{-4} \times T^2 + 0.1529 \times T + 5.72$	0.99
0.1 %	$\varepsilon'' = 2 \times 10^{-4} \times T^2 + 0.1360 \times T + 9.28$	0.99
0.2 %	$\varepsilon'' = 2 \times 10^{-4} \times T^2 + 0.1904 \times T + 10.63$	0.99
0.5 %	$\varepsilon'' = 7 \times 10^{-4} \times T^2 + 0.2386 \times T + 16.13$	0.99
1.0 %	$\varepsilon'' = 1.2 \times 10^{-3} \times T^2 + 0.3361 \times T + 27.42$	0.99
2.0 %	$\varepsilon'' = -1 \times 10^{-3} \times T^2 + 0.9162 \times T + 32.81$	0.97
Rice		
0.0 %	$\varepsilon'' = 2 \times 10^{-4} \times T^2 - 0.0307 \times T + 7.54$	0.98
0.2 %	$\varepsilon'' = 4 \times 10^{-4} \times T^2 - 0.0181 \times T + 7.81$	0.99
0.5 %	$\varepsilon'' = -3 \times 10^{-4} \times T^2 + 0.0623 \times T + 9.43$	0.99
1.0 %	$\varepsilon'' = 4 \times 10^{-5} \times T^2 + 0.1571 \times T + 11.85$	0.99
1.5 %	$\varepsilon'' = -7 \times 10^{-6} \times T^2 + 0.3444 \times T + 14.58$	0.99
2.0 %	$\varepsilon'' = -6 \times 10^{-5} \times T^2 + 0.6508 \times T + 16.23$	0.99

234 kPa was maintained inside the MATS system to prevent breakage of the seals of the food packages. For each product, samples of the same thickness and two different salt contents were processed in one experimental run. For each test condition, three sensors were placed in the food packages to record the temperature profiles at the cold spot. Each test was conducted in duplicates.

3.3.2. Determination of the heating patterns

The experimental heating patterns inside the food samples processed with the MATS system were determined based on the chemical marker M-2 formed in the browning reaction between D-ribose and amino acids during the thermal treatments. With the help of a computer vision assistance technique, the brown color formed during heating was converted to a set of RGB (red, green and blue) values. The more heated areas turned red, while the medium and less heated areas turned green and blue, respectively (Pandit et al., 2007).

3.4. Statistical analysis

MATLAB with Statistics Toolbox software version 2022a (Natick, MA, USA) was used to develop the charts and perform statistical analyses. The adequacy of the correlation between the prediction from the charts and the experimental values was determined by evaluating the lack of fit and the coefficient of determination (R^2) of the linear regression. For the linear regression the experimental values (y-axis) were plotted against the predicted values (x-axis) as described by Piñeiro et al. (2008). The statistical significance of the models and standardized residuals were evaluated at the 5% probability level ($P < 0.05$).

4. Results and discussion

4.1. Chart development

4.1.1. Relationships between temperature and the dielectric properties of food samples

First, the relationship between temperature and loss factor was established at different salt contents for the selected products (Table 1). Based on the equations, Fig. 3 was established for mashed potato samples to create the first half of the chart.

Fig. 3 illustrates the effect of salt content and temperature on the increase of the loss factor in the mashed potato samples. Salt content increase results in higher dissolved ions, which enhances ionic conductivity to increase the loss factor. Additionally, the rise in product temperature increased the dissolved ions mobility, resulting in the rise of the loss factor (İcier and Baysal, 2004; Ryynänen, 1995; Tang, 2015). A similar pattern is also observed in pea and rice products (Figs. 7 and 8) (Jain et al., 2019).

Likewise, the relationship between temperature (20–120 °C) and dielectric constant was established at six different salt contents for the three food samples (Table 2). The dielectric constant, which indicates the ability of food to store electric energy, is also influenced by the

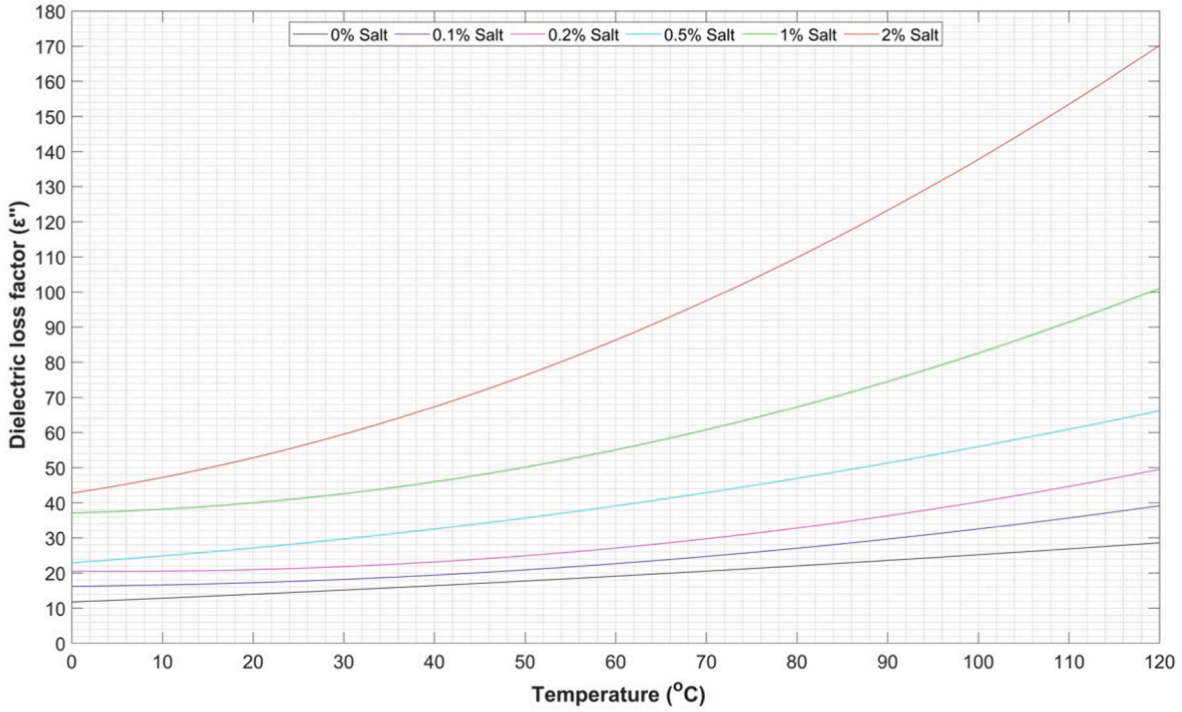

Fig. 3. Relationships between temperature and loss factor for mashed potato samples at different salt contents.

Table 2
Relationships between temperature,T (20–120 °C) and the dielectric constant at different salt contents, (n = 3).

Salt content	Correlations	R^2
Mashed Potatoes		
0.0 %	$\varepsilon' = 7 \times 10^{-4} \times T^2 - 0.2161 \times T + 70.98$	0.99
0.1 %	$\varepsilon' = 1 \times 10^{-3} \times T^2 - 0.2715 \times T + 71.53$	0.99
0.2 %	$\varepsilon' = 11 \times 10^{-4} \times T^2 - 0.2934 \times T + 73.69$	0.99
0.5 %	$\varepsilon' = 1 \times 10^{-3} \times T^2 - 0.2696 \times T + 72.58$	0.99
1.0 %	$\varepsilon' = 14 \times 10^{-4} \times T^2 - 0.3243 \times T + 74.54$	0.99
2.0 %	$\varepsilon' = 7 \times 10^{-4} \times T^2 - 0.1946 \times T + 71.73$	0.99
Peas		
0.0 %	$\varepsilon' = -1 \times 10^{-4} \times T^2 - 0.0714 \times T + 59.43$	0.99
0.1 %	$\varepsilon' = 4 \times 10^{-4} \times T^2 - 0.1325 \times T + 59.13$	0.99
0.2 %	$\varepsilon' = 8 \times 10^{-4} \times T^2 - 0.2289 \times T + 65.92$	0.99
0.5 %	$\varepsilon' = 1 \times 10^{-4} \times T^2 - 0.0979 \times T + 62.66$	0.99
1.0 %	$\varepsilon' = 0 \times 10^{-4} \times T^2 - 0.0657 \times T + 61.00$	0.99
2 .0%	$\varepsilon' = 3 \times 10^{-4} \times T^2 - 0.1068 \times T + 61.70$	0.99
Rice		
0.0 %	$\varepsilon' = 4 \times 10^{-4} \times T^2 - 0.1635 \times T + 65.45$	0.99
0.2 %	$\varepsilon' = 6 \times 10^{-4} \times T^2 - 0.2193 \times T + 65.78$	0.99
0.5 %	$\varepsilon' = 6 \times 10^{-4} \times T^2 - 0.2250 \times T + 69.65$	0.99
1.0 %	$\varepsilon' = 8 \times 10^{-4} \times T^2 - 0.2471 \times T + 67.37$	0.99
1.5 %	$\varepsilon' = -4 \times 10^{-4} \times T^2 - 0.0632 \times T + 62.19$	0.99
2.0 %	$\varepsilon' = -1 \times 10^{-4} \times T^2 - 0.0907 \times T + 67.04$	0.99

temperature and salt content. In general, it slightly increases with increasing salt content and decreases with increasing temperature (İcier and Baysal, 2004; Ryynänen, 1995).

4.1.2. Relationship between dielectric properties, thickness, and heating rates

Following the logical flow of the loop iteration presented in Fig. 4 and using MATLAB software, the heating rates of mashed potatoes were calculated for different thicknesses and salt contents. Using Eq. (12), derived from Eqs. (10) and (11), the loss factors (y-axis) were plotted against the estimated heating rates (x-axis) of the mashed potatoes to create the second half of the chart, as presented in Fig. 5. This figure consists of 36 heating rate curves for six thickness levels (16, 18, 20, 23, 25 and 28 mm) and six salt content levels (0, 0.1, 0.2, 0.5, 1 and 2%). Fig. 5 shows the influence of temperature, dielectric properties, thickness and volumetric specific heat on the heating rates in the central layer of mashed potatoes. Heating curves start at 0 °C and end at 120 °C which is a sterilization temperature. The volumetric specific heat used in the calculations was 3.8, 4.7 and 3 MJ/(°C·m^3) for mashed potato, pea and rice samples, respectively, where the respective densities are 1.1 × 10^3, 1.3 × 10^3, and 0.96 × 10^3 kg/m^3 (Jain et al., 2019).

$$\varepsilon'' = \frac{\rho C_P}{2\pi f \varepsilon_o |E|^2}\left(\frac{dT}{dt}\right) \tag{12}$$

The black dashed lines (Fig. 5) are drawn with known fixed dielectric constant values that range from 50 to 70 with an interval of 5 (50:5:70). These fixed lines can be used as a reference to track the change in the dielectric constant values as the temperature increases in the mashed potato samples.

4.1.3. Construction of the charts

Finally, the two sets of graphs in Figs. 3 and 5 were superimposed with the MATLAB software to form the chart for mashed potatoes, as shown in Fig. 6. Eq. (13) was used to combine the first and second parts of the chart using the loss factor as a common variable. This approach allows to relate the product temperature (T) to its heating rate (dT/dt). Similarly, charts for pea and rice samples were developed as presented

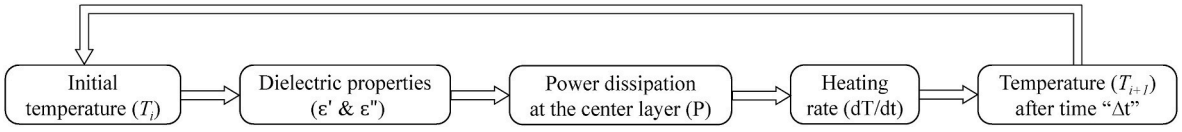

Fig. 4. Loop iteration for the heating rate prediction (adapted from Gezahegn et al. (2023)).

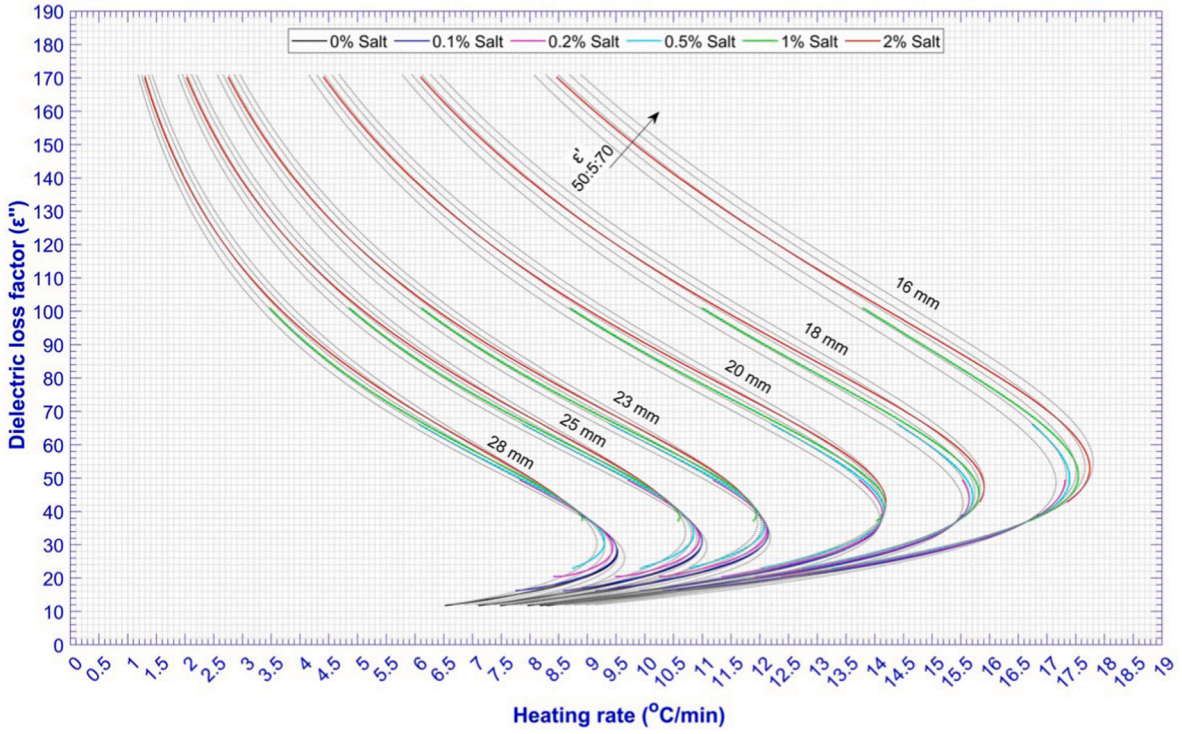

Fig. 5. Relationship among the heating rates, dielectric properties and thickness at different salt contents of mashed potato samples processed in the MATS system.

in Figs. 7 and 8, respectively. As presented by Gezahegn et al. (2023), the newly developed analytical charts are named as Gezahegn-Tang (G-T) charts. The G-T charts relate the complex relationship among temperature, dielectric properties, thickness, salt content, and heating rate in the central layer of the food processed in the MATS system. Fig. 8 shows the lowest heating rate of rice samples with 0% salt content. Other authors also reported the lower heating rate and loss factors of rice samples with 0% salt content in 915 MHz microwaves (Auksornsri et al., 2018; Jain

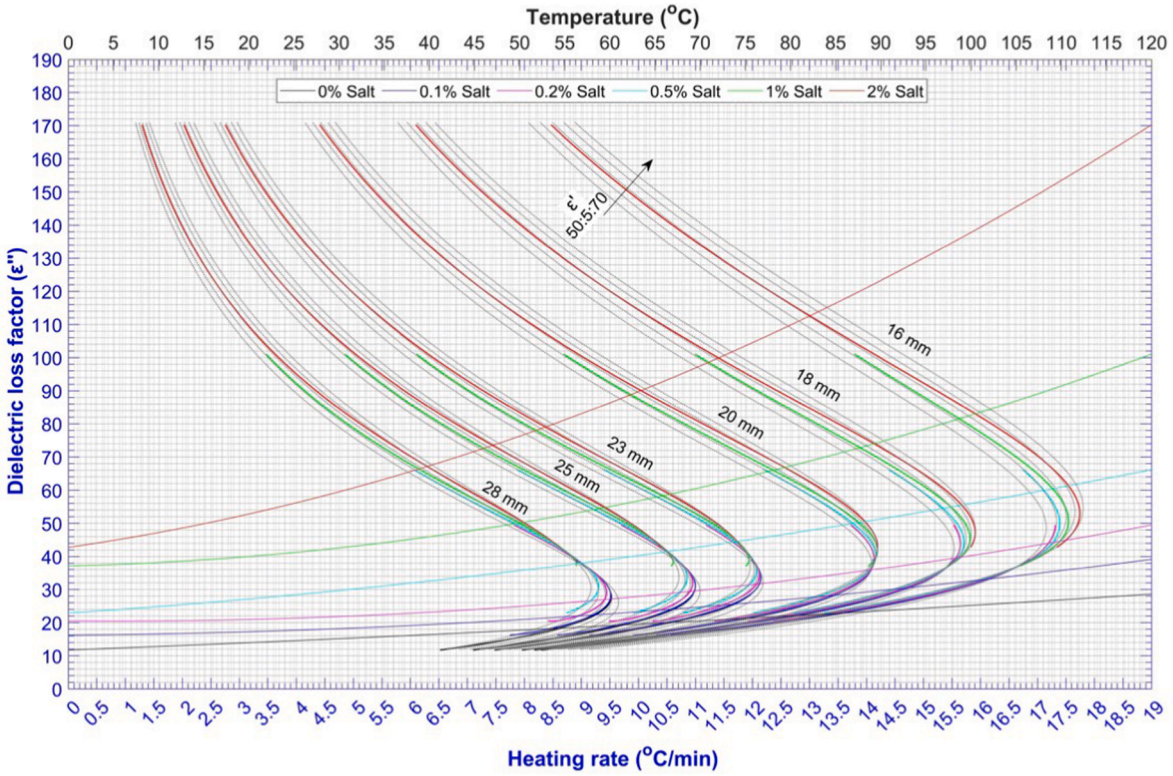

Fig. 6. G-T chart for the mashed potato samples in the MATS system.

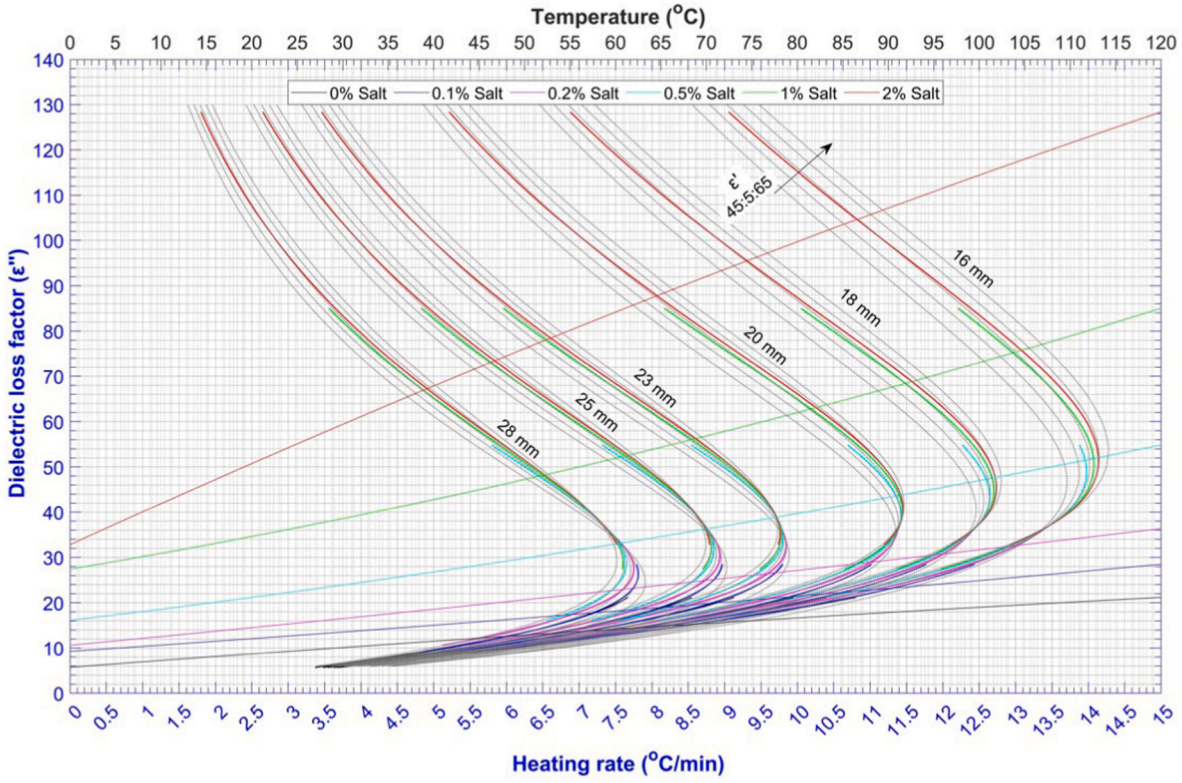

Fig. 7. G-T chart for the pea samples in the MATS system.

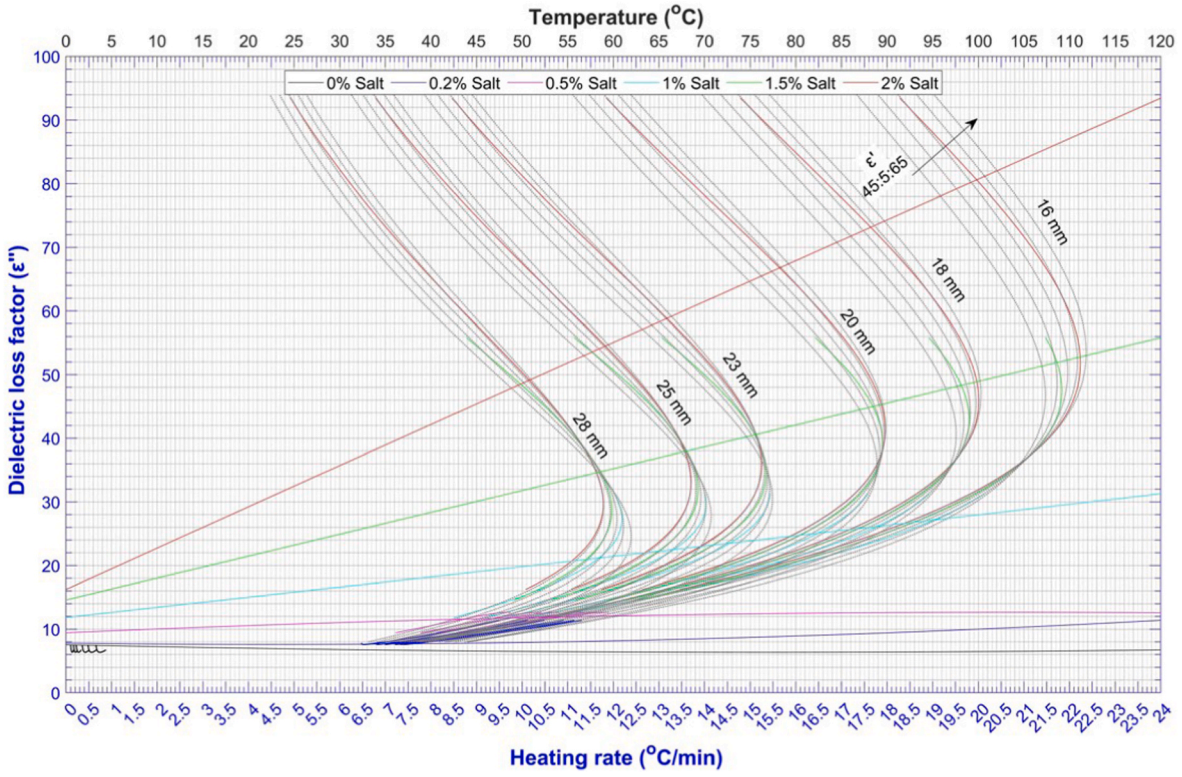

Fig. 8. G-T chart for the rice samples in the MATS system.

et al., 2019; Gezahegn et al., 2023).

$$\underbrace{aT^2 + bT + c = \varepsilon''}_{\text{First half of the G−T chart}} = \underbrace{\frac{\rho C_P}{2\pi f \varepsilon_o |E|^2}\left(\frac{dT}{dt}\right)}_{\text{Second half of the G−T chart}} \tag{13}$$

4.2. Experimental validation for the charts

4.2.1. Heating temperature

For validation of the chart predictions which are obtained using the loop iterations (Fig. 4), experimental runs were conducted using mashed potatoes with various salt contents (0, 0.1, 0.2, 0.5, 1, and 2%) and thicknesses (16, 20, 23 and 28 mm). After being preheated to 60–62 °C, the samples were processed in the microwave heating section of the MATS system for 4.6 min. During the heating stage, 138 temperature data were taken at 2-s intervals. Fig. 9 shows the correlations between the predicted and the experimental temperatures of various samples with different salt contents and thicknesses. Due to the displacement of the food packages through the microwave heating cavities, the experimental temperatures show a wavy pattern. The maximum microwave heating (electric field intensity) occurs at the center of the cavities, whereas the minimums occur at the entrance and exit of the cavities (Luan et al., 2016). The results show that the experimental observations fit the predicted values within the 95% confidence interval and with R^2 from 0.94 to 0.99.

The experimental and predicted average heating rates of mashed potatoes with 0.1% salt content and different thicknesses were compared in Fig. 10. The average heating rates were calculated by dividing the differences between the preheating and final temperature by the heating time (4.6 min). In the experimental observations and the predicted values, samples with less thickness (16 mm) were heated faster than the thicker samples (23 and 28 mm). The results show an agreement between the G-T chart predictions and the experimental heating rate values.

4.2.2. Optimal salt content

The charts can accurately predict the optimal salt content for a maximum heating rate in the three products. As explained in Sections 4.3.2, the optimal salt content that yields the highest heating rate can be indicated by identifying the ranges of the heating rate curves of a sample at different salt contents. The optimal salt content differs for various thicknesses and heating temperature ranges.

According to the chart, the optimal salt content for 23 mm thick mashed potato samples heated from 60 to 120 °C is found to be 0.1%. With the same heating condition, the optimal salt content for pea with 18 mm thickness was 0.5%, and for rice with 25 mm thickness was 1%. As depicted in Fig. 11, the experimental results confirm that the chart predictions for the optimal salt content for the maximum heating rate are accurate.

At their respective optimal salt contents, the three food samples show an intense red color that indicates the highest heating rate. The green and blue colors correspond to the medium and lowest heating rates, respectively. Note that the experimental heating pattern results can only be used within a sample to compare across various salt contents. The results cannot be used for comparison among different samples because of the difference in the background color of the food matrices and the chemical marker (M-2) formation rate between the samples.

The intensity of the red color in each product heating pattern image (Fig. 11) also agreed with the magnitude of the heating rates presented in Tables 3–5. For mashed potatoes, the order of salt contents that gives

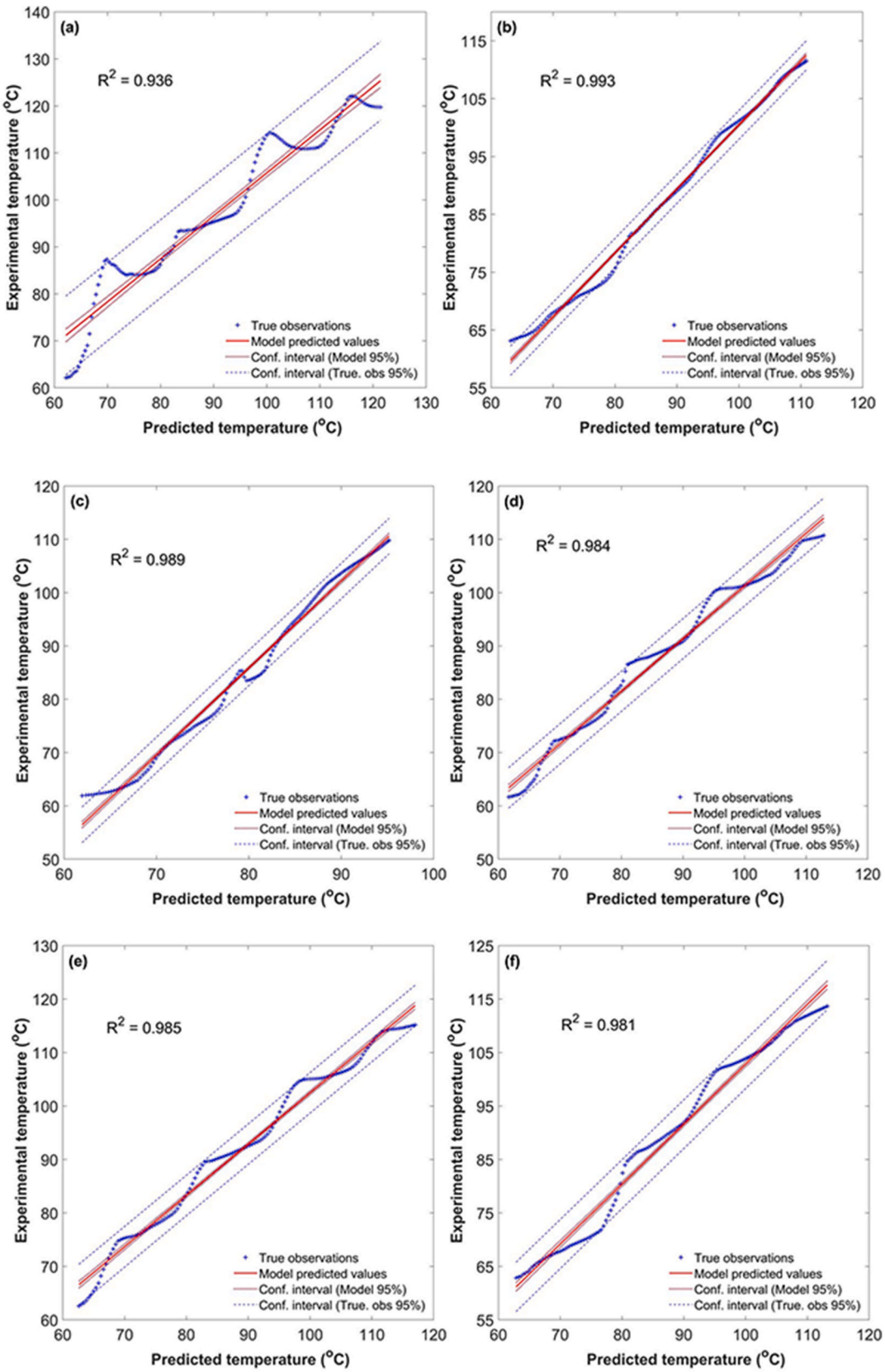

Fig. 9. Correlation between the predicted and experimental temperatures of mashed potatoes: 20 mm thick with 0.1% (a), 1% (b) and 2% (c) salt contents; 23 mm thick with 0% (d), 0.2% (e) and 0.5% (f) salt contents. The central line corresponds to the regression model; the dotted lines (....) represent the 95% confidence interval for the regression, and the dashed lines (– –) represent the 95% confidence interval for the experimental values.

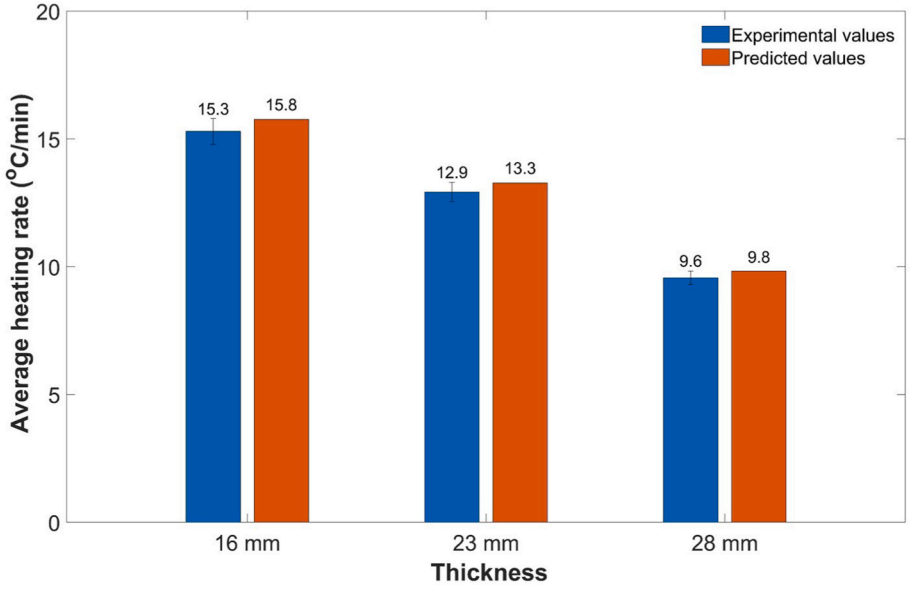

Fig. 10. The average heating rates of mashed potatoes of different thicknesses with 0.1% salt content.

the highest heating rate to the lowest was: 0.1% (11.872 °C/min), 0.2% (11.871 °C/min), 0% (11.3 °C/min), 0.5% (10.9 °C/min), 1% (8.5 °C/min), and 2% (4.9 °C/min). For peas, the order of salt contents was: 0.5% (12.5 °C/min), 0.2% (11.7 °C/min), 1% (11.5 °C/min), 0.1% (10.8 °C/min), 0% (9.3 °C/min), and 2% (8.4 °C/min). In rice products, the order was: 1% (13.8 °C/min), 1.5% (12.7 °C/min), 0.5% (12.2 °C/min), 2% (9.1 °C/min), 0.2% (8.7 °C/min), and 0% (0.2 °C/min).

4.3. Chart applications

4.3.1. Predicting the average heating rate and time

To find a heating rate of a product at specific salt content and thickness, users can identify the product's initial temperature and its loss factor from the first half of the chart. From the second half of the chart, the corresponding heating rate to the loss factor can be obtained

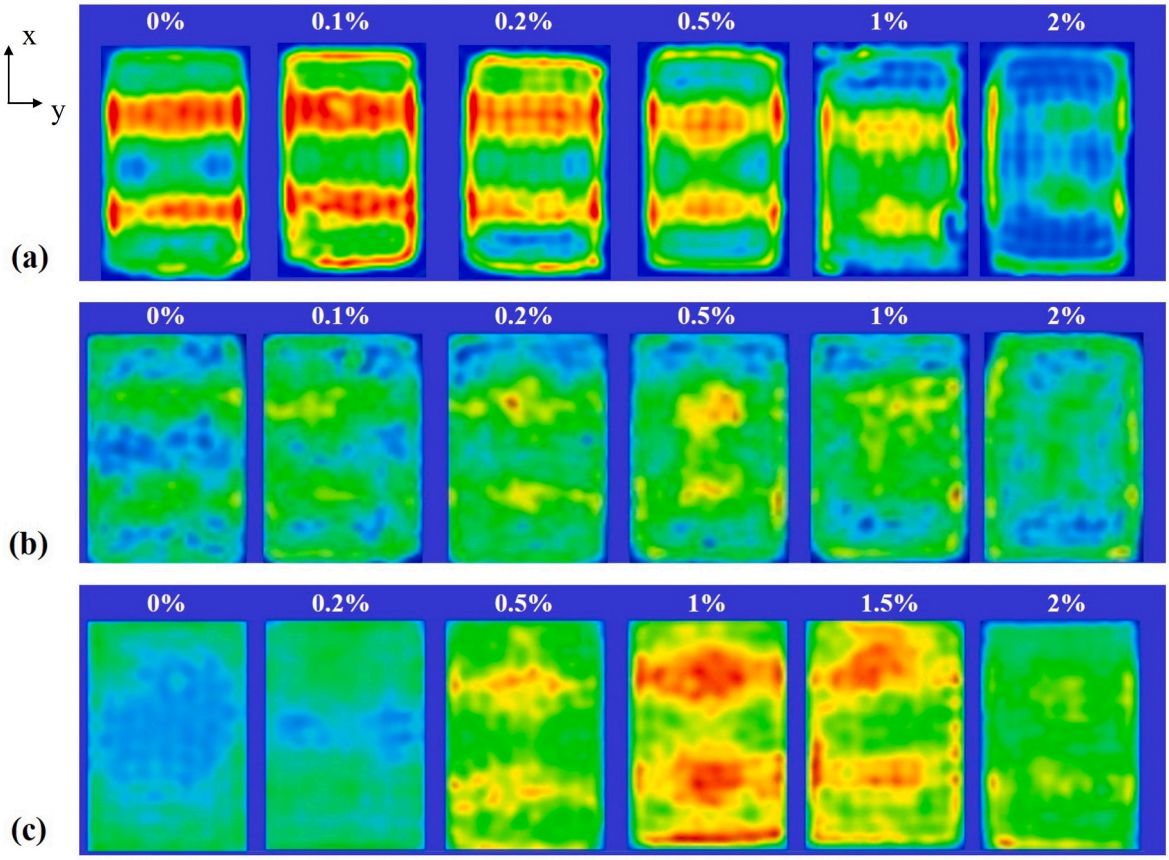

Fig. 11. Experimental heating patterns at the central layer of mashed potato (a), pea (b) and rice (c) samples. The dimensions of the products area were 140 × 95 mm. The percentages indicating the salt contents on (b) and (c) were adapted from Jain et al. (2019).

Table 3
Heating rates and times for mashed potato samples of different thicknesses at different salt contents.

Thickness	Salt content (%)	Heating rate (°C/min)				Heating time (min)
		At 60 °C	At 120 °C	Average approx	Average Integral	
16 mm	0.0	12.0	15.2	13.6	13.7	4.4
	0.1	13.4	16.9	15.2	15.4	3.9
	0.2	14.7	17.3	16.0	16.4	3.7
	0.5	16.9	16.7	17.0	17.2	3.5
	1.0	17.5	13.8	15.6	16.0	3.7
	2.0	15.6	8.5	12.0	12.0	5.0
18 mm	0.0	11.6	14.4	13.0	13.2	4.6
	0.1	12.9	15.5	14.2	14.5	4.1
	0.2	14.0	15.5	15.3	15.2	4.0
	0.5	15.6	14.4	15.4	15.3	3.9
	1.0	15.5	11.0	13.2	13.5	4.4
	2.0	12.8	6.1	9.5	9.3	6.4
20 mm	0.0	11.2	13.5	12.3	12.5	4.8
	0.1	12.3	14.1	13.2	13.5	4.5
	0.2	13.1	13.7	13.8	13.9	4.3
	0.5	14.2	12.2	13.2	13.5	4.4
	1.0	13.5	8.7	11.1	11.3	5.3
	2.0	10.4	4.4	7.4	7.2	8.3
23 mm	0.0	10.3	12.0	11.1	11.3	5.3
	0.1	11.1	12.0	11.9	11.9	5.1
	0.2	11.7	11.2	11.8	11.9	5.1
	0.5	12.0	9.4	10.7	10.9	5.5
	1.0	10.8	6.1	8.4	8.5	7.0
	2.0	7.6	2.8	5.2	4.9	12.2
25 mm	0.0	9.7	11.0	10.3	10.5	5.7
	0.1	10.4	10.7	10.7	10.8	5.5
	0.2	10.8	9.7	10.6	10.6	5.6
	0.5	10.7	7.9	9.3	9.5	6.3
	1.0	9.2	4.9	7.0	7.1	8.5
	2.0	6.2	2.0	4.1	3.8	15.6
28 mm	0.0	8.8	9.5	9.4	9.3	6.5
	0.1	9.2	8.9	9.3	9.3	6.4
	0.2	9.4	7.8	9.2	9.0	6.7
	0.5	8.9	6.1	7.5	7.6	7.9
	1.0	7.4	3.5	5.4	5.4	11.1
	2.0	4.6	1.3	3.0	2.7	22.3

Table 4
Heating rates and times for pea samples of different thicknesses at different salt contents.

Thickness	Salt content (%)	Heating rate (°C/min)				Heating time (min)
		At 60 °C	At 120 °C	Average approx	Average Integral	
16 mm	0.0	8.1	10.8	9.5	9.6	6.3
	0.1	9.8	12.6	11.2	11.2	5.3
	0.2	11.0	13.4	12.2	12.4	4.8
	0.5	13.0	13.9	13.8	13.7	4.4
	1.0	14.1	12.2	13.1	13.4	4.5
	2.0	12.6	9.2	10.9	10.7	5.6
18 mm	0.0	7.9	10.4	9.2	9.3	6.5
	0.1	9.5	11.9	10.7	10.8	5.6
	0.2	10.6	12.4	11.5	11.7	5.1
	0.5	12.2	12.3	12.4	12.5	4.8
	1.0	12.6	10.0	11.3	11.5	5.2
	2.0	10.5	7.1	8.8	8.4	7.1
20 mm	0.0	7.7	9.9	8.8	8.9	6.7
	0.1	9.1	11.1	10.1	10.2	5.9
	0.2	10.0	11.4	10.7	10.9	5.5
	0.5	11.2	10.7	11.2	11.2	5.3
	1.0	11.0	8.2	9.6	9.7	6.2
	2.0	8.6	5.4	7.0	6.6	9.1
23 mm	0.0	7.3	9.1	8.2	8.3	7.2
	0.1	8.5	9.8	9.2	9.3	6.5
	0.2	9.1	9.8	9.7	9.7	6.2
	0.5	9.8	8.5	9.6	9.4	6.4
	1.0	8.9	6.0	7.4	7.5	8.0
	2.0	6.3	3.6	4.9	4.6	13.0
25 mm	0.0	6.9	8.5	7.7	7.9	7.6
	0.1	8.0	9.0	8.5	8.6	7.0
	0.2	8.5	8.8	8.8	8.8	6.8
	0.5	8.8	7.3	8.1	8.3	7.3
	1.0	7.7	4.8	6.3	6.3	9.6
	2.0	5.2	2.8	4.0	3.7	16.4
28 mm	0.0	6.4	7.7	7.1	7.2	8.4
	0.1	7.3	7.8	7.7	7.7	7.8
	0.2	7.6	7.4	7.6	7.6	7.9
	0.5	7.6	5.8	6.7	6.8	8.8
	1.0	6.2	3.6	4.9	4.8	12.4
	2.0	3.8	1.9	2.9	2.6	23.1

(Gezahegn et al., 2023). As the example shows in Fig. 12, start from the initial temperature, move downward (arrow a-1 or b-1) until the intersection with the curve for the specific salt content, then move horizontally (arrow a-2 or b-2) until the intersection with the corresponding heating rate curve of the specific salt content and thickness, and finally move downward (arrow a-3 or b-3) to read the heating rate from the blue horizontal axis. From the identified heating rate at initial/preheating temperature (with arrow a-3 or b-3), it is possible to estimate the required heating time by dividing the temperature gain (from initial to final temperature) by the heating rate as shown in Eq. (14). However, since the heating rate is non-constant throughout the heating process, estimating a heating time by only considering the heating rate at the initial temperature will result in inaccurate result. Hence, it will be essential to take the average heating rate that occurs from the start to the end of the heating process. For example (Fig. 12, arrow "b"), mashed potatoes with 20 mm thickness and 1% salt content have an initial heating rate of 13.5 °C/min at 60 °C (see arrows b-1, b-2 and b-3) and the final heating rate of 10.5 °C/min at 100 °C (see arrows b-4, b-5 and b-6); therefore, the time required to heat the product from 60 to 100 °C can be calculated by dividing the temperature gain (40 °C) by the average heating rate (12.0 °C/min), which estimates a heating time of 3.33 min. In a validation experiment, heating the same product from 61.5 to 100 °C took 3.30 min, only a 1.8-sec difference from the estimated value.

$$Time\ required = \frac{T_{final} - T_{initial}}{dT/dt} \tag{14}$$

Depending on the nature of the product, salt content, thickness, etc., some products may not have a straight heating rate line, as discussed in the above example with arrow "b." Different scenarios are given in Fig. 13, where the heating rate line is curved. In such cases, we can find the average heating rate (approximate) using Eq. (15), which assumes the heating rate curves as a linear line. To be more precise, the integral average under the curve of the heating rate lines can be calculated. The integral average heating rate values and their respective required heating time for the three food products are given in Tables 3–5, which are almost similar to the heating rates calculated with Eq. (15).

$$Average\ heating\ rate\ (approximate) = \frac{(a + 3b + 2c)}{6} \tag{15}$$

where a and c represent the minimum and the maximum heating rate values respectively (°C/min); b represents either the final (Fig. 13 (a)) or the initial (Fig. 13 (b)) heating rate (°C/min).

Let us consider an example with a curved heating rate line (Fig. 13 (b)). Mashed potato with 23 mm thickness and 0.2% salt content has an initial heating rate (b) of 11.7 °C/min at 60 °C (see arrows a-1, a-2 and a-3), a final heating rate (a) of 11.4 °C/min at 115 °C (see arrows a-4, a-5 and a-6), and a maximum heating rate (c) of 12.1 °C/min (see arrow a-7). The average heating rate can be calculated according to Eq. (15), which is 11.8 °C/min. The time required to heat the product from 60 to 115 °C can be calculated by diving the temperature gain (55 °C) by the average heating rate (11.8 °C/min). The heating time required is 4.66 min. In the validation experiment, heating the same product from 62.6 to 115.2 °C took 4.60 min, with only 3.6-sec variation, given an initial temperature difference of 2.6 °C.

Tables 3–5 summarize the heating rates of mashed potato, pea, and

Table 5
Heating rates and times for rice samples of different thicknesses at different salt contents.

Thickness	Salt content (%)	Heating rate (°C/min)				Heating time (min)
		At 60 °C	At 120 °C	Average approx	Average Integral	
16 mm	0.0	0.7	0.9	0.8	0.8	76.8
	0.2	7.7	11.4	9.5	9.6	6.2
	0.5	12.3	16.8	14.5	14.9	4.0
	1.0	16.5	20.2	18.3	18.7	3.2
	1.5	20.5	21.5	21.5	21.6	2.8
	2.0	22.2	18.5	20.4	20.5	2.9
18 mm	0.0	0.6	0.7	0.6	0.6	101.7
	0.2	7.6	11.2	9.4	9.5	6.3
	0.5	12.0	16.2	14.1	14.4	4.2
	1.0	15.9	19.0	17.4	17.8	3.4
	1.5	19.1	19.1	19.3	19.5	3.1
	2.0	19.6	15.1	17.4	17.3	3.5
20 mm	0.0	0.4	0.5	0.5	0.4	134.7
	0.2	7.5	11.0	9.2	9.3	6.4
	0.5	11.6	15.4	13.5	13.9	4.3
	1.0	15.1	17.6	16.4	16.7	3.6
	1.5	17.7	16.6	17.6	17.5	3.4
	2.0	17.1	12.1	14.6	14.5	4.1
23 mm	0.0	0.3	0.3	0.3	0.3	205.5
	0.2	7.3	10.5	8.9	9.0	6.7
	0.5	11.0	14.2	12.6	12.9	4.7
	1.0	13.9	15.4	15.2	15.0	4.0
	1.5	15.3	13.3	14.3	14.5	4.1
	2.0	13.7	8.7	11.2	10.9	5.5
25 mm	0.0	0.2	0.3	0.2	0.2	272.2
	0.2	7.1	10.2	8.6	8.7	6.9
	0.5	10.5	13.3	11.9	12.2	4.9
	1.0	13.0	14.0	13.8	13.8	4.4
	1.5	13.9	11.4	12.6	12.7	4.7
	2.0	11.7	7.0	9.4	9.1	6.6
28 mm	0.0	0.1	0.2	0.2	0.1	415.5
	0.2	6.8	9.5	8.2	8.3	7.2
	0.5	9.8	11.9	10.8	11.1	5.4
	1.0	11.7	12.0	12.0	12.1	5.0
	1.5	11.8	9.0	10.4	10.4	5.8
	2.0	9.4	5.1	7.2	6.9	8.7

rice products at 60 °C (close to the initial product temperature in MATS) and 120 °C (close to the sterilization temperature). The average heating rates, approximate and integral, were calculated with Eq. (15) and using MATLAB software, respectively. The required heating times were obtained by dividing the temperature gain (60 °C), from the preheating to the final sterilization temperature, by the integral average heating rates.

4.3.2. *Determining the optimal salt content for the maximum heating rate*

The optimum salt content (for a maximum heating rate) of a product can be identified from the G-T chart, given the product thickness and the heating temperature range (initial/preheating and final/sterilization temperature). As described in Section 4.3.1, once the heating rate curves of a sample are identified for all different salt contents within the specific heating temperature range, users can identify the salt content that yields the maximum average heating rate or the minimum heating time. Figs. 14–16 show the ranges of the heating rate curves for mashed potato, pea and rice products with different thicknesses and salt contents for heating temperatures ranging from 60 to 120 °C. For simplicity, the dashed dielectric constant lines, the loss factor lines (from the first half of the chart), and the heating rate lines (from the second half of the chart) that range from 0 to 60 °C were omitted from Figs. 14–16.

As shown in Fig. 14, mashed potato products with 16 and 18 mm thicknesses and with 0.5% salt content have the maximum heating rate compared to other salt levels. 0.2% salt content for 20 mm products and 0.1% salt content for 23–28 mm products were found to be optimum salt contents for higher heating rates. Similar facts are reported in Table 3, where the minimum heating times, 3.5 min for 16 mm thick sample and 3.9 min for 18 mm thick sample, were obtained at 0.5% salt content. For 20 mm thick products, the minimum time, 4.3 min, occurred at 0.2% salt content; for 23, 25 and 28 mm thick products, the minimum heating times, 5.1, 5.5 and 6.4 min, were found at 0.1% salt content, respectively.

Fig. 15 presents the optimal salt contents for peas, where products with 16–20 mm thicknesses and with 0.5% salt content have maximum heating. Products with 23–25 mm thicknesses have a maximum heating rate at 0.2% salt content, and 28 mm thick products have an optimal salt content of 0.1%. Also, Table 4 shows that the minimum heating times of 4.4 min (for 16 mm), 4.8 min (for 18 mm), and 5.3 min (for 20 mm) were obtained at 0.5% salt content. For 23 and 25 mm thick products, the minimum times, 6.2 and 6.8 min, respectively, occurred at 0.2% salt content. For 28 mm thick products, the minimum heating time, 7.8 min, was found at 0.1% salt content.

As depicted in Fig. 16, rice products with 16–20 mm thicknesses and with 1.5% salt content have the maximum heating rate compared with other salt contents; for 23–28 mm thick products, 1% was found to be the optimum salt content. Matching facts are presented in Table 5, where the minimum heating times, 2.8 min (for 16 mm), 3.1 min (for 18 mm), and 3.4 min (for 20 mm), were obtained at 1.5% salt content. For products with 23, 25 and 28 mm thicknesses, the minimum heating times, 4.0, 4.4, and 5.0 min, respectively, occurred at 1% salt content.

In all the three products, the values of the optimum salt contents decrease as the product thickness increases. This fact might be due to the decay of microwave power (conversion to thermal energy) while traveling from the surface to the center of the food. Power decay before the power reaches the center of the product will cause higher heating at the surface than at the center. Since the main contributing factors for microwave power decay are the dipole rotation of water molecules and conduction of dissolved ions from the added salt, more added salt in the products will result in higher power loss in the surface layer or less power absorption in the center layer of a product (Hong et al., 2021a,b; Ryynänen, 1995; Tang, 2015). Hence, recipe formulation with less salt is recommended for products with higher thicknesses to avoid lower heating at the center or more power decay in the surface layer.

Moreover, the maximum heating rate at the center of a certain thickness product increases with the level of the salt content to a certain level. However, a reduction in the heating rate was observed beyond the optimum salt content. This fact might be due to the absorption of more microwave power by the added salt in the food surface layer than at the center. The same observation was reported by Jain et al. (2019) and Hong et al. (2021a,b). Hence, additional salt content beyond the optimal is not advisable to ensure adequate center heating.

Different engineering charts can be developed for various products with a similar approach, as discussed in Section 4. In this research, mashed potato, pea and rice were selected to represent different categories of food products, i.e., vegetable, legume, and cereal, respectively. Since most RTE meals are composed of various ingredients, the availability of multiple G-T charts for different kinds of products will be helpful for process engineers in the development of process schedules. In the application of the engineering charts for products with multiple ingredients, the food that possesses the lowest average heating rate (longest heating time) can be taken as a worst-case scenario to develop the process schedules according to FDA (2016) and IFTPS (2014).

If there is a change in the MATS circulating water (tap or purified water) or input power from the generators, the E_0 shall be determined to get an accurate estimation of the heating rate. As Gezahegn et al. (2021) discussed, circulating purified water minimizes the microwave power decay within the circulating water, resulting in higher heating rates in prepackaged foods. According to Eq. (10), a change in E_0 value will alter the heating rate by the power of two. The E_0 can be determined using Eq. (13), Eq. (2), and experimental measurement of the heating temperature (T), heating rate (dT/dt), dielectric properties and volumetric specific heat of the food. Other technologies that use microwave energy as the main heating source can also apply a similar approach to develop an engineering chart. Regardless of the technology, the first half of the

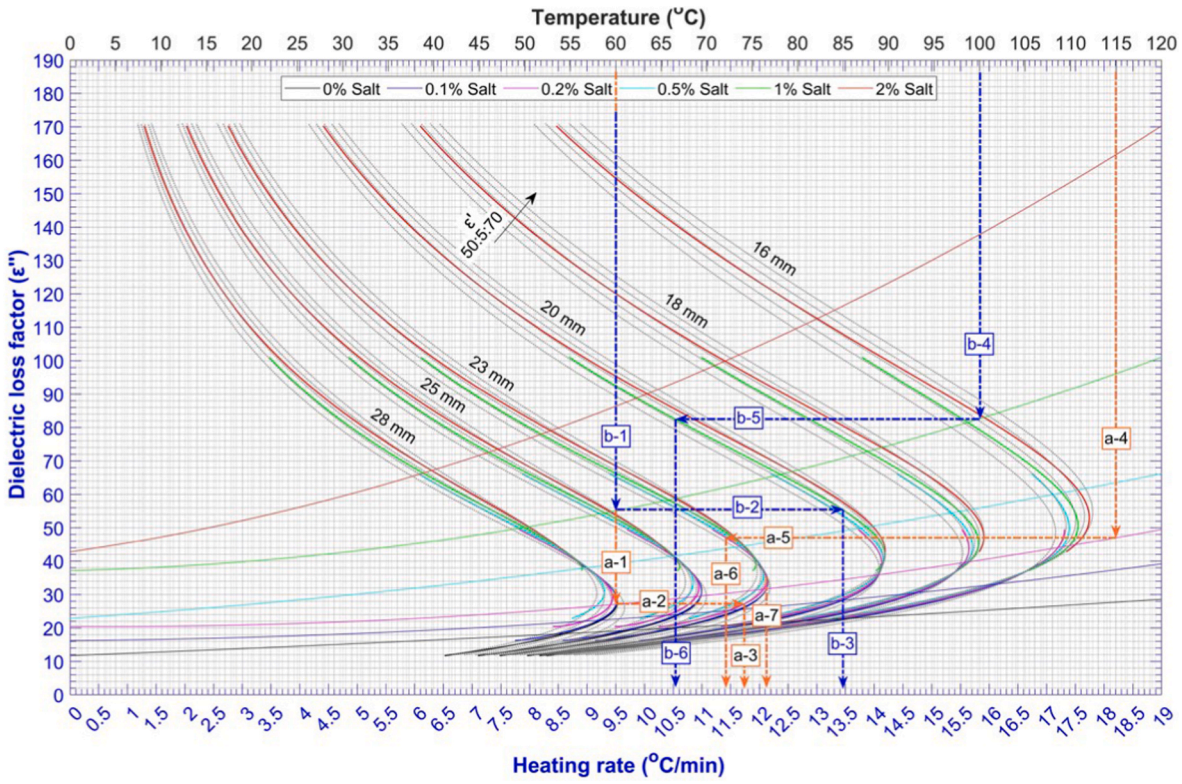

Fig. 12. Heating rate and heating time prediction for the mashed potato samples in the MATS system.

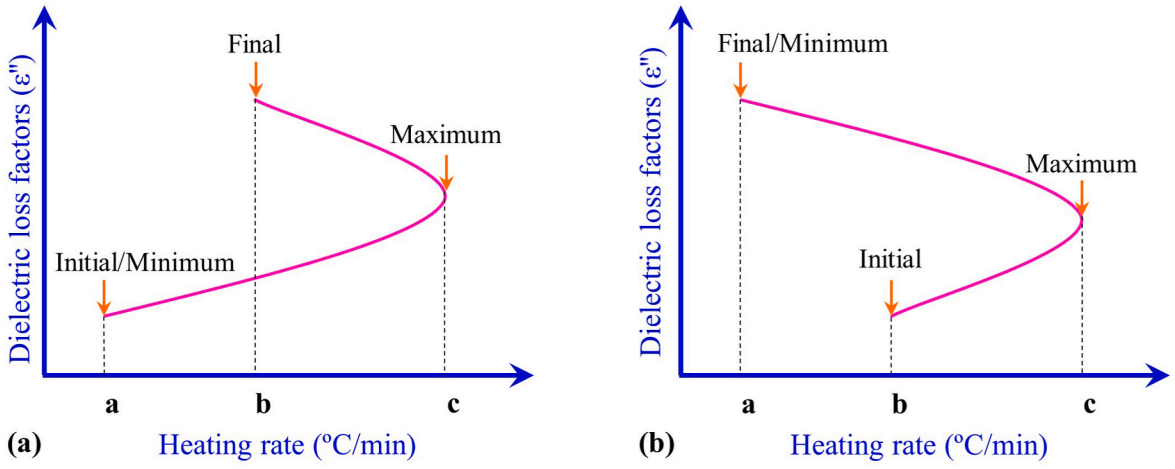

Fig. 13. Different scenarios for the heating rate curve: (a) the initial heating rate is lower than the final heating rate, and (b) the final heating rate is lower than the initial heating rate.

chart (loss factor *vs*. temperature lines) can be used as it is. Nevertheless, the second half of the chart should be determined for each specific system (loss factor *vs*. heating rate curves), not based on a MATS system.

5. Conclusion

Engineering charts for mashed potato, pea and rice samples were developed by applying Maxwell's and heat transfer equations. The charts show the relationships among the food dielectric properties, the food thicknesses, the heating temperatures and heating rates at the cold spot of the food product processed in the MATS system. Three distinct charts were developed for mashed potato, pea and rice samples. Important information about a product, such as the dielectric properties, the heating rate and time, and the optimal salt content (formulation) for the maximum heating rate, can be acquired from the charts. The charts were validated by experimental runs with the 915-MHz single-mode MATS system installed at WSU. The predicted and experimental temperature profiles at the cold spots of the mashed potato samples correlated well, with a R^2 ranging from 0.94 to 0.99. Additionally, the predicted optimal salt contents for maximum heating rates agreed with the experimental heating pattern results for all the three food products. In the future, similar G-T charts can be developed for other types of food products. Using the charts should significantly save time and resources in developing MATS sterilization process schedules at the industrial level.

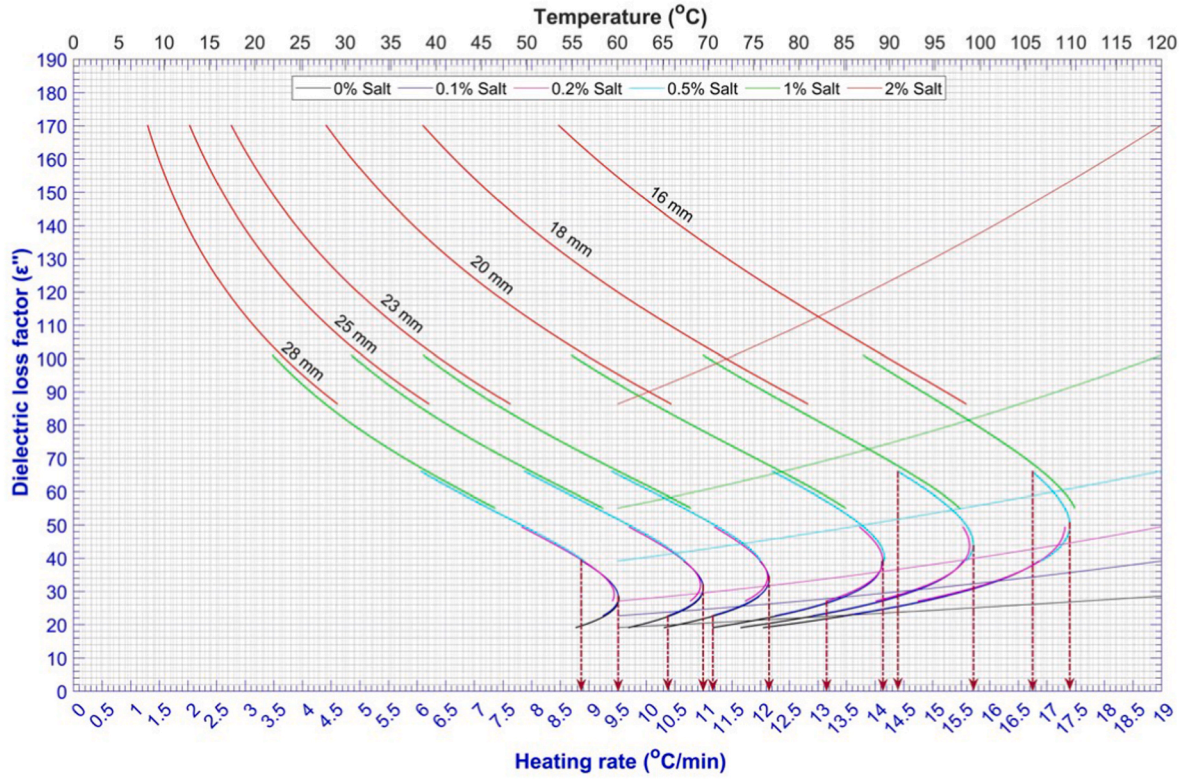

Fig. 14. Optimal salt content determination for mashed potato samples while heating from 60 to 120 °C in the MATS system.

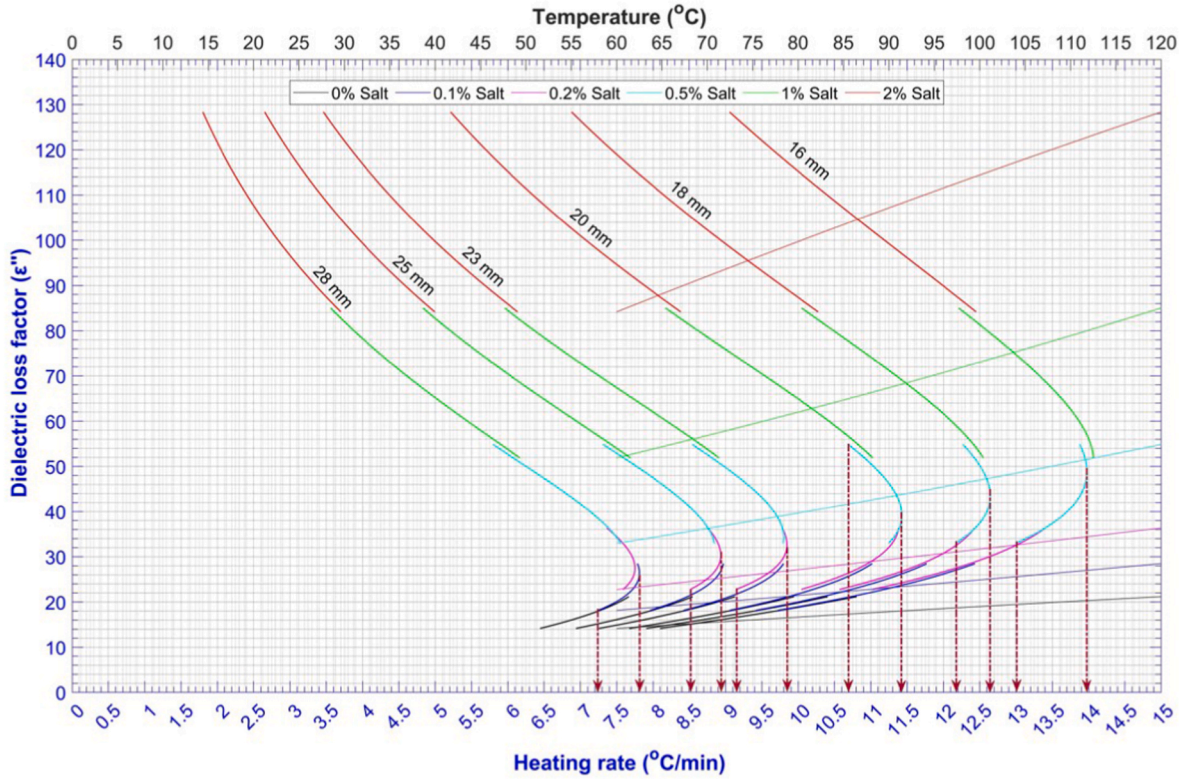

Fig. 15. Optimal salt content determination for pea samples while heating from 60 to 120 °C in the MATS system.

CRediT authorship contribution statement

Yonas Gezahegn: Conceptualization, Methodology, Investigation, Validation, Data curation, Formal analysis, Software, Writing – original draft, Writing – review & editing, Visualization, Project administration. **Juming Tang:** Conceptualization, Methodology, Writing – review & editing, Funding acquisition, Resources, Supervision, Project administration. **Patrick Pedrow:** Conceptualization, Writing – review & editing.

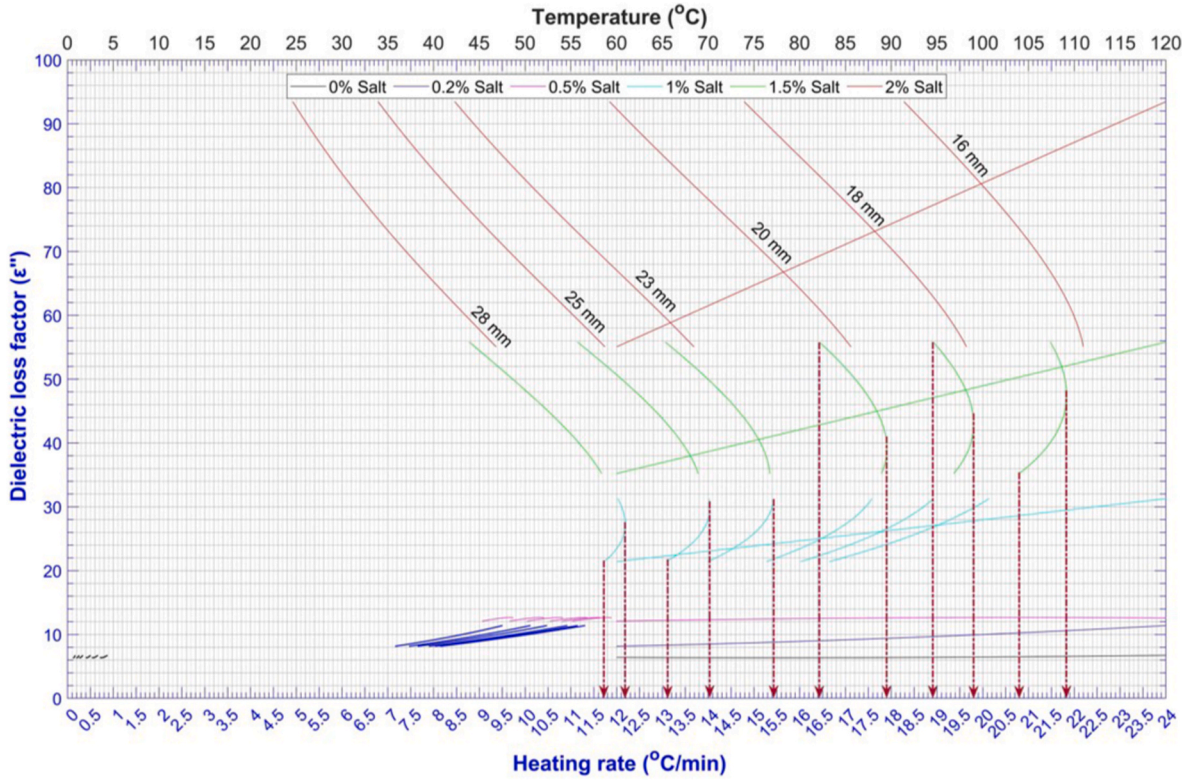

Fig. 16. Optimal salt content determination for rice samples while heating from 60 to 120 °C in the MATS system.

Shyam S. Sablani: Conceptualization, Writing – review & editing. **Zhongwei Tang:** Investigation, Data curation, Writing – review & editing. **GustavoV. Barbosa-Cánovas:** Conceptualization, Writing – review & editing.

Declaration of competing interest

- All authors have participated in (a) conception and design, or analysis and interpretation of the data; (b) drafting the article or revising it critically for important intellectual content; and (c) approval of the final version.
- This research article is original, and neither submitted nor under review for publication elsewhere.
- Its publication is approved by all authors and tacitly or explicitly by the responsible authorities where the work was carried out and sponsored.
- If accepted, it will not be published elsewhere in the same form, in English or in any other language, including electronically without the written consent of the copyright-holder.

Data availability

Data will be made available on request.

Acknowledgments

The authors would like to acknowledge the support of the USDA: National Institute of Food and Agriculture grant [#2016-68003- 24840] and the Washington State University: Hatch project [#1016366].

References

Auksornsri, T., Tang, J., Tang, Z., Lin, H., Songsermpong, S., 2018. Dielectric properties of rice model food systems relevant to microwave sterilization process. Innovat. Food Sci. Emerg. Technol. 45, 98–105. https://doi.org/10.1016/j.ifset.2017.09.002.

Balanis, C.A., 2012. Advanced Engineering Electromagnetics, second. John Wiley & Sons, Inc, NJ.

Chizoba Ekezie, F.-G., Sun, D.-W., Han, Z., Cheng, J.-H., 2017. Microwave-assisted food processing technologies for enhancing product quality and process efficiency: a review of recent developments. Trends Food Sci. Technol. 67, 58–69. https://doi.org/10.1016/j.tifs.2017.05.014.

FDA, 2016. Center for Food Safety and Applied Nutrition. Hazard Analysis and Risk-Based Preventive Controls for Human Food: Guidance for Industry. Department of Health and Human Services.

Gezahegn, Y., Tang, J., Sablani, S.S., Pedrow, P.D., Hong, Y.-K., Lin, H., Tang, Z., 2021. Dielectric properties of water relevant to microwave assisted thermal pasteurization and sterilization of packaged foods. Innovat. Food Sci. Emerg. Technol. 74, 102837 https://doi.org/10.1016/j.ifset.2021.102837.

Gezahegn, Y., Hong, Y.-K., Tang, J., Pedrow, P., Sablani, S.S., Liu, F., Tang, Z., 2023. Development and validation of analytical charts for microwave assisted thermal pasteurization of selected food products. J. Food Eng. 349, 111434 https://doi.org/10.1016/j.jfoodeng.2023.111434.

Hillier-Brown, F.C., Summerbell, C.D., Moore, H.J., Wrieden, W.L., Adams, J., Abraham, C., et al., 2017. A description of interventions promoting healthier ready-to-eat meals (to eat in, to take away, or to be delivered) sold by specific food outlets in England: a systematic mapping and evidence synthesis. BMC Publ. Health 17 (1), 93. https://doi.org/10.1186/s12889-016-3980-2.

Hong, Y.-K., Liu, F., Tang, Z., Pedrow, P.D., Sablani, S.S., Yang, R., Tang, J., 2021b. A Simplified Approach to Assist Process Development for Microwave Assisted Pasteurization of Packaged Food Products. Innovative Food Science & Emerging Technologies, 102628. https://doi.org/10.1016/j.ifset.2021.102628.

Hong, Y.-K., Stanley, R., Tang, J., Bui, L., Ghandi, A., 2021a. Effect of electric field distribution on the heating Uniformity of a model ready-to-eat meal in microwave-assisted thermal sterilization using the FDTD method. Foods 10 (2), 311. https://doi.org/10.3390/foods10020311.

İcier, F., Baysal, T., 2004. Dielectrical properties of food materials—1: factors affecting and industrial uses. Crit. Rev. Food Sci. Nutr. 44 (6), 465–471. https://doi.org/10.1080/10408690490886692.

IFTPS (Institute For Thermal Processing Specialists), 2014. Guidelines for Conducting Thermal Processing Studies. Guelph, ON. Canada.

Jain, D., Tang, J., Pedrow, P.D., Tang, Z., Sablani, S., Hong, Y.-K., 2019. Effect of changes in salt content and food thickness on electromagnetic heating of rice, mashed potatoes and peas in 915 MHz single mode microwave cavity. Food Res. Int. 119 (August), 584–595. https://doi.org/10.1016/j.foodres.2018.10.036.

Luan, D., Tang, J., Pedrow, P.D., Liu, F., Tang, Z., 2013. Using mobile metallic temperature sensors in continuous microwave assisted sterilization (MATS) systems. J. Food Eng. 119 (3), 552–560. https://doi.org/10.1016/j.jfoodeng.2013.06.003.

Luan, D., Tang, J., Pedrow, P.D., Liu, F., Tang, Z., 2015. Performance of mobile metallic temperature sensors in high power microwave heating systems. J. Food Eng. 149, 114–122. https://doi.org/10.1016/j.jfoodeng.2014.09.041.

Luan, D., Tang, J., Pedrow, P.D., Liu, F., Tang, Z., 2016. Analysis of electric field distribution within a microwave assisted thermal sterilization (MATS) system by computer simulation. J. Food Eng. 188, 87–97. https://doi.org/10.1016/j.jfoodeng.2016.05.009.

Pandit, R.B., Tang, J., Liu, F., Mikhaylenko, G., 2007. A computer vision method to locate cold spots in foods in microwave sterilization processes. Pattern Recogn. 40 (12), 3667–3676. https://doi.org/10.1016/j.patcog.2007.03.021.

Pandit, R.B., Tang, J., Mikhaylenko, G., Liu, F., 2006. Kinetics of chemical marker M-2 formation in mashed potato—a tool to locate cold spots under microwave sterilization. J. Food Eng. 76 (3), 353–361. https://doi.org/10.1016/j.jfoodeng.2005.05.032.

Piñeiro, G., Perelman, S., Guerschman, J.P., Paruelo, J.M., 2008. How to evaluate models: observed vs. predicted or predicted vs. observed? Ecol. Model. 216 (3–4), 316–322. https://doi.org/10.1016/j.ecolmodel.2008.05.006.

Remnant, J., Adams, J., 2015. The nutritional content and cost of supermarket ready-meals. Cross-sectional analysis. Appetite 92, 36–42. https://doi.org/10.1016/j.appet.2015.04.069.

Resurreccion, F.P., Tang, J., Pedrow, P., Cavalieri, R., Liu, F., Tang, Z., 2013. Development of a computer simulation model for processing food in a microwave assisted thermal sterilization (MATS) system. J. Food Eng. 118 (4), 406–416. https://doi.org/10.1016/j.jfoodeng.2013.04.021.

Ryynänen, S., 1995. The electromagnetic properties of food materials: a review of the basic principles. J. Food Eng. 26 (4), 409–429. https://doi.org/10.1016/0260-8774(94)00063-F.

Tang, J., 2015. Unlocking potentials of microwaves for food safety and quality. J. Food Sci. 80 (8), E1776–E1793. https://doi.org/10.1111/1750-3841.12959.

Tang, J., Hong, Y.-K., Inanoglu, S., Liu, F., 2018. Microwave pasteurization for ready-to-eat meals. Curr. Opin. Food Sci. 23, 133–141. https://doi.org/10.1016/j.cofs.2018.10.004.

Tang, J., Liu, F., Pathak, K., Eves, E., 2006. U.S. Patent No. 7,119. Pullman, Washington: U.S. Patent, p. 313.

Thienhirun, S., Chung, S., 2018. Consumer Attitudes and Preferences toward cross-cultural ready-to-eat (RTE) food. J. Food Prod. Market. 24 (1), 56–79. https://doi.org/10.1080/10454446.2016.1266544.

Yoon, E., 2017. The Grocery industry confronts a new Problem: only 10% of Americans Love cooking. Harvard Business Review. Retrieved from. https://hbr.org/2017/09/the-grocery-industry-confronts-a-new-problem-only-10-of-americans-love-cooking.

Zhang, W., Tang, J., Liu, F., Bohnet, S., Tang, Z., 2014. Chemical marker M2 (4-hydroxy-5-methyl-3(2H)-furanone) formation in egg white gel model for heating pattern determination of microwave-assisted pasteurization processing. J. Food Eng. 125, 69–76. https://doi.org/10.1016/j.jfoodeng.2013.10.020.